Molecular Dynamics Simulation of the Proline Conformational Equilibrium and Dynamics in Antamanide Using the GROMOS Force Field

R. M. Brunne, W. F. van Gunsteren,* R. Brüschweiler, and R. R. Ernst*

Contribution from the Laboratorium für Physikalische Chemie, Eidgenössische Technische Hochschule, 8092 Zürich, Switzerland

Received November 16, 1992

Abstract: Molecular dynamics simulations of the proline-containing cyclic peptide antamanide using the GROMOS force field have been performed in order to compare the conformational equilibrium and dynamics of the four proline residues with experimental data originating from NMR spectroscopy. *J*-coupling constants, order parameters, and conformational populations are well-reproduced. The average simulated conformational residence times of 4 ps are shorter than the measured ones which are on the order of 30 ps, implying a somewhat too flexible force field for proline rings. The proline dynamics seems to be insensitive to the observed conformational dynamics of the peptide ring and to the solvent viscosity.

1. Introduction

Molecular dynamics simulations have proven to be successful in refining structures obtained from NMR spectroscopy or X-ray crystallography.[1,2] For small and medium-size molecules, one often finds in this way the relevant low-energy conformations and can reproduce the population numbers in good agreement with experimental data. Nevertheless, the dynamics of the interconversion among different conformations is yet a challenge to the application of force field methods.

The goal of this paper is to test, by means of an example, whether the general force field of GROMOS is able to correctly reproduce the experimentally derived conformational equilibrium distribution and to qualitatively describe the conformational dynamics. We have chosen the phenomenon of proline ring flips within the cyclic decapeptide antamanide, *cyclo*-(-Val[1]-Pro[2]-Pro[3]-Ala[4]-Phe[5]-Phe[6]-Pro[7]-Pro[8]-Phe[9]-Phe[10]-), Figure 1, as an example for the rapid conformational process for which experimental data are available.

This work should be seen in the context of a more extended effort to study the possibilities of combined molecular dynamics and NMR investigations of intramolecular processes.

The structure of antamanide[3-6] as well as the dynamics of the backbone[7-9] and the side chain rotations[9] have been studied extensively in solution by various methods. An overview of the literature on antamanide is given by Kessler et al.[5] Recently, Mádi et al.[10] presented a detailed analysis of NMR data with respect to the proline ring flips. They found that Pro[2] and Pro[7] interconvert rapidly between two energetically similar conformations,[11] while Pro[3] and Pro[8] dominantly occupy one conformation in accordance with the general rules formulated by Cung et al.[12]

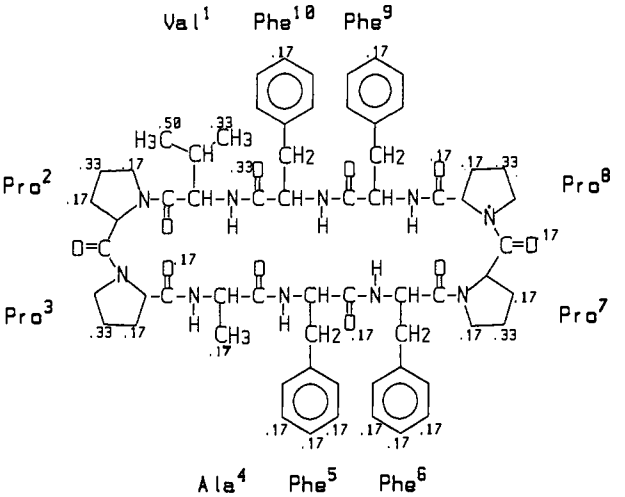

Figure 1. Primary structure of antamanide. Non-zero atomic accessible area weight factors ω_i for a representative conformation are listed with the (united) atoms.

For the simulation, we chose the stochastic dynamics (SD) method[13,14] rather than standard molecular dynamics to describe antamanide dissolved in chloroform. In this way we do not have to treat the solvent molecules explicitly, but can include the influence of the nonpolar solvent in the frictional and the random forces of the Langevin equation of motion:

$$m_i\, \mathrm{d}v_i(t)/\mathrm{d}t = F_i(\{x_i(t)\}) - m_i\gamma_i v_i(t) + R_i(t) \qquad (1)$$

The acceleration $\mathrm{d}v_i/\mathrm{d}t$ of atom i with mass m_i is determined by the force F_i resulting from the atomic force field, and by the friction term with the friction coefficient γ_i and the random force R_i, which both mimic the interactions with the solvent. It has been shown[14] that stochastic dynamics yields a good approximation

(1) McCammon, J. A.; Harvey, S. C. *Dynamics of Proteins and Nucleic Acids*; Cambridge University Press: London, 1987.
(2) van Gunsteren, W. F.; Berendsen, J. H. C. *Angew. Chem., Int. Ed. Engl.* **1990**, *29*, 992.
(3) Kessler, H.; Müller, A.; Oschkinat, H. *Magn. Reson. Chem.* **1985**, *23*, 844.
(4) Kessler, H.; Griesinger, C.; Lautz, J.; Müller, A.; van Gunsteren, W. F.; Berendsen, H. J. C. *J. Am. Chem. Soc.* **1988**, *110*, 3393.
(5) Kessler, H.; Müller, A.; Pook, K.-H. *Liebigs Ann.* **1989**, 903.
(6) Kessler, H.; Bats, J. W.; Lautz, J.; Müller, A. *Liebigs Ann.* **1989**, 913.
(7) Patel, D. J. *Biochemistry* **1973**, *12*, 667.
(8) Burgermeister, W.; Wieland, T.; Winkler, R. *Eur. J. Biochem.* **1974**, *44*, 305.
(9) Burgermeister, W.; Wieland, T.; Winkler, R. *Eur. J. Biochem.* **1974**, *44*, 311.
(10) Mádi, Z. L.; Griesinger, C.; Ernst, R. R. *J. Am. Chem. Soc.* **1990**, *112*, 2908.
(11) Shekar, S. C.; Easwaran, K. R. K. *Biopolymers* **1982**, *21*, 1479.
(12) Cung, M. T.; Vitoux, B.; Marraud, M. *New J. Chem.* **1987**, *11*, 503.
(13) van Gunsteren, W. F.; Berendsen, H. J. C. *Mol. Simulation* **1988**, *1*, 173.
(14) Shi, Y.-y.; Wang, L.; van Gunsteren, W. F. *Mol. Simulation* **1988**, *1*, 369.

0002-7863/93/1515-4764$04.00/0

of the full solvent effects on the solute properties in the case of nonpolar solvents.

2. Methods

For the SD simulation we used the GROMOS program library[15] and standard GROMOS force field.[15] The correlation functions of the uncorrelated random forces $R_i(t)$ in eq 1 are related to the friction coefficients γ_i by

$$\langle R_i(0)R_j(t)\rangle = 2m_i\gamma_i k_B T_{ref}\delta_{ij}\delta(t) \quad (2)$$

where k_B denotes Boltzmann's constant and T_{ref} the reference temperature of the solvent bath. The friction coefficients γ_i for the solute atoms are determined from Stokes' law

$$\gamma = \frac{6\pi r_s \eta_s}{m_s} \quad (3)$$

and

$$\gamma_i = \omega_i \gamma \quad (4)$$

where r_s is Stokes' radius, m_s is the mass and η_s the viscosity of the solvent, and ω_i is an atomic accessible area weight factor that is chosen to approximate the relative surface area of each solute atom that is accessible to solvent.[14] The accessible surface area weight factor ω_i of a given solute atom i is set to 1 if this atom has no neighboring solute atoms within a distance of 0.3 nm and is stepwise reduced to zero until the number of neighboring solute atoms within 0.3 nm reaches 6. Typical ω_i values are shown in Figure 1.

Although the NMR data were obtained in chloroform, we mimicked the solvent using available force field data of the related molecule carbon tetrachloride. The Stokes' radius for the CCl_4 united atom was derived from the Lennard-Jones parameters[16] and set to r_s = 0.296 nm. From this, the mass of carbon tetrachloride (m_s = 153.823 amu) and the viscosity (η_s = 0.00881 P (at 300 K)),[17] eq 3 yields a solvent friction coefficient (γ) of 19 ps^{-1}.

We started our simulations from a structure derived from NMR data.[18] First this structure was energy-minimized using the steepest descent method (440 steps) followed by the conjugate gradients method[19] (102 steps). In the latter procedure, a new conjugate gradient cycle was started every 50 steps. The step size was chosen between 0.01 and 0.05 nm in both cases. We kept all bond lengths constrained within 10^{-3} relative to the reference lengths using the SHAKE method.[20] Here, as well as in all subsequent simulations, the cutoff distance for pair interactions was set to 10 nm. In this way, all atomic pairs were included.

In a second step, the minimized structure was equilibrated during 10 ps of stochastic dynamics simulation at the reference temperature of 300 K. Initial velocities were taken from a Maxwell-Boltzmann velocity distribution at 300 K, the time step increment was 2 fs, SHAKE was applied with a relative bond length tolerance of 10^{-4}, and the temperature coupling constant for the coupling to a heat bath[21] was changed from 0.01 to 0.1 ps after the first picosecond and kept at this value for all subsequent simulations.

From this point, a first simulation 500 ps in length was performed with γ = 19 ps^{-1}. During this initial period, we observed torsional angle transitions in the backbone part of the cyclic peptide. From this state, three simulations with different friction coefficients were done to analyze the dynamics of the proline puckering. Simulation **A** was continued for another 500 ps using γ = 19 ps^{-1}, and the atomic friction coefficients γ_i was calculated according to eq 4 with the accessible surface area of each solute atom. Simulation **B** started from the same coordinates as run **A** with newly assigned velocities from a Maxwell–Boltzmann velocity distribution at 300 K and also continued for 500 ps. Here, the solvent friction coefficient was set equal to γ = 100 ps^{-1}. A third simulation of 500 ps, **C**, started from the same initial state, but now the atomic friction coefficient was kept constant at γ_i = 20 ps^{-1} for every solute (united) atom irrespective of its accessible surface area.

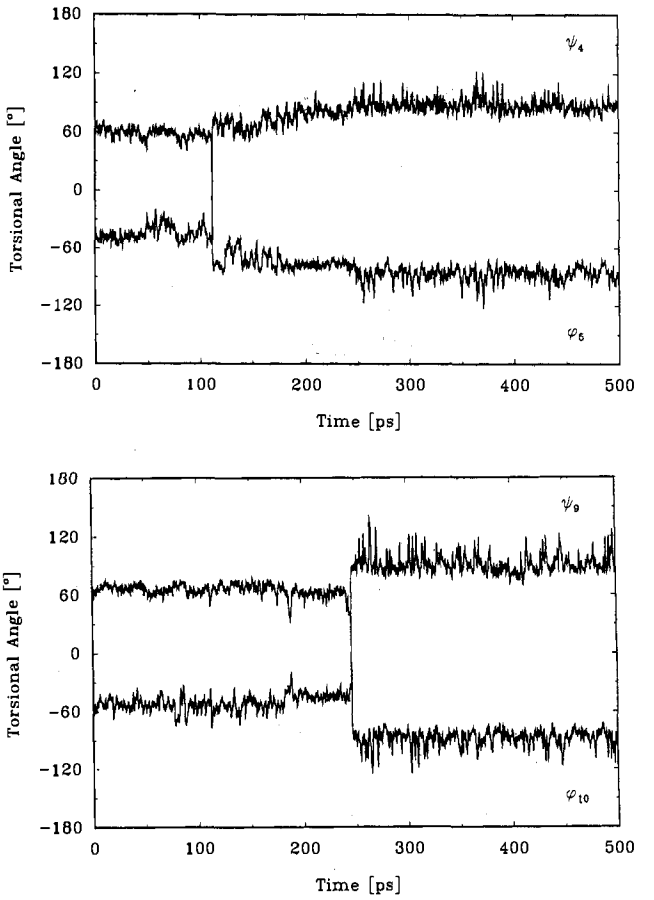

Figure 2. (a) Trajectories for the backbone torsional angles of ψ(Ala^4) and ϕ(Phe^5) showing the peptide bond unit rotation after 110 ps of SD simulation **A**. (b) Trajectories for the backbone torsional angles of ψ-(Phe^9) and ϕ(Phe^{10}) showing the peptide bond unit rotation after 240 ps of SD simulation **A**.

3. Results

Only during the first 500-ps simulation did we observe conformational transitions within the backbone of antamanide. Three out of four conformations, proposed before to explain NMR data,[4,6] were identified. They result from concerted rotations about the peptide bonds connecting residues Ala^4 with Phe^5 and Phe^5 with Phe^6 on the one hand and residues Phe^9 with Phe^{10} and Phe^{10} with Val^1 on the other. As can be seen from Figure 2a, the torsional angles involved in the turn of the peptide unit Ala^4-Phe^5 change after 110 ps from approximately ψ_4/ϕ_5 = −45°/+60° (conformation I) to +90°/−90° (conformation II). At the same time, ψ_5/ϕ_6 changes from −50°/−45° to +85°/−130°. After 240 ps the torsional angles ψ_9/ϕ_{10} undergo transitions from −55°/+65° (conformation II) to +90°/−90° (conformation III), as exemplified in Figure 2b, while ψ_{10}/ϕ_1 changes at the same time from −50°/−40° to +80°/−110°.

The observed proline ring flips cause all intraresidue torsional angles to change at the same time. Taking the change of the χ_2 angles with time as representative, we can group Pro^2 and Pro^7 into one group of similar behavior and Pro^3 and Pro^8 into another. While Pro^2 and Pro^7 exhibit transitions between two conformations and remain in each for several picoseconds, Pro^3 and Pro^8 attempt transitions from a more stable to an energetically unfavorable conformation with a lifetime that hardly ever exceeds 1 ps. In Figure 3 the trajectories of the χ_2 angles of Pro^7 and Pro^8 are given as examples.

(15) van Gunsteren, W. F.; Berendsen, H. J. C. *Groningen Molecular Simulation (GROMOS) Library Manual*; Biomos: Groningen, 1987.
(16) Rebertus, D. W.; Berne, B. J.; Chandler, D. *J. Chem. Phys.* **1979**, *70*, 3395.
(17) Weast, R. C., Ed. *Handbook of Chemistry and Physics*, 56th ed.; CRC Press: Boca Raton, 1982.
(18) Brüschweiler, R.; Blackledge, M.; Ernst, R. R. *J. Biomol. NMR* **1991**, *1*, 3.
(19) Fletcher, R.; Reeves, C. M. *Comput. J.* **1964**, *7*, 149.
(20) Ryckaert, J.-P.; Ciccotti, G.; Berendsen, H. J. C. *J. Comput. Phys.* **1977**, *23*, 327.
(21) Berendsen, H. J. C.; Postma, J. P. M.; van Gunsteren, W. F.; DiNola, A.; Haak, J. R. *J. Chem. Phys.* **1984**, *81*, 3684.

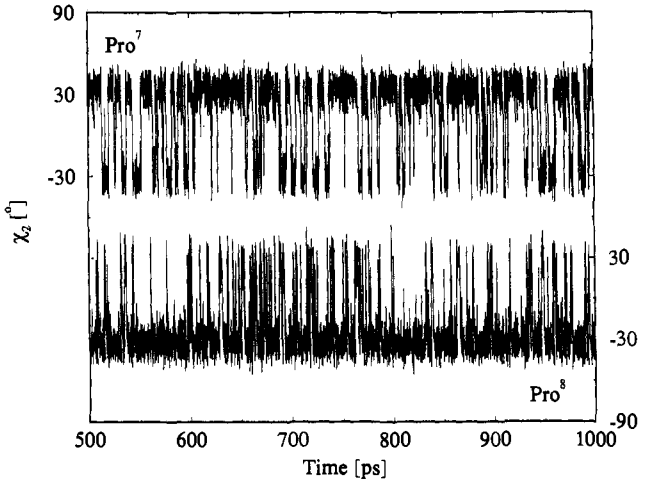

Figure 3. Trajectories of the χ_2 angles of Pro^7 (left-hand scale) and Pro^8 (right-hand scale) taken from SD simulation A.

There is no significant correlation observable between the backbone conformation and the populations and mean torsional χ_2 angles, as can be inferred from Table I. Yet, we analyze the proline dynamics in detail only for the second half of the 1-ns simulations that does not show any backbone transitions.

The two conformations of each proline can be characterized by the χ_2 angle which experiences the largest change during the conformational transition. Proline configurations with $\chi_2 > 0°$ were assigned to one conformer and those with $\chi_2 < 0°$ to the other. Remigration, that is a transition from one conformer to the other immediately followed by a back-transition, is not accounted for. For each conformation of the four prolines, average torsional angles are computed. The results for run A are collected in Table II together with the results from NMR spectroscopy[10] and from X-ray data.[22]

The vicinal proton–proton coupling constants $^3J_{HH}$ within the proline residues were calculated according to a modified Karplus relation[23,24]

$$^3J_{HH} = a_1 \cos^2\theta + a_2 \cos\theta + a_3 + \sum \Delta x_i\{a_4 + a_5 \cos^2(\xi_i\theta + a_6|\Delta x_i|)\} \quad (5)$$

where θ is the HC–CH dihedral angle. The coefficients a_1 through a_6 depend on the substituents[23,24] attached to the HC–CH fragment, taking into account the electronegativity[25] (Δx_i) of these substituents and their substituents and considering an orientation parameter (ξ_i) for the position of the substituents.[26] The results of this analysis are given in Table III. There is a qualitative agreement between the SD and NMR results, although it is apparent that for Pro^2 and Pro^7 the range of values is larger for SD than for NMR, while the situation is opposite for Pro^3 and Pro^8. A perfect agreement is indeed not expected as the GROMOS force field parameters have not been specifically optimized for proline residues.

In addition, we calculated the jump angles $\Delta\Theta$ of the ^{13}C–H bond vectors for the ring-flip process for each carbon center. This allowed us then to determine the order parameter S^2 in a two-site model that can be used to explain the observed carbon-13 NMR relaxation times.[10]

To calculate the intramolecular jump angles $\Delta\Theta$ for the ^{13}C–H vectors of the prolines, it is necessary to eliminate the overall molecular rotation using the well-justified assumption of independent overall and internal motion. For this purpose, a residue-fixed coordinate system was defined by the carbonyl C atoms of proline and the preceding residue and the center of the proline N–C_α bond. For each conformer-trajectory the coordinates with respect to the residue-fixed coordinate system are averaged and for every carbon center the position of a *pro-R*-H atom (for the C_α atom the position of the H atom) is calculated. The jump angle $\Delta\Theta$ is then given by the angle between the mean C–H vectors of the two conformations. It allows the determination of the order parameter S^2 which enters into the ^{13}C relaxation rate constant T_1^{-1}.[11] For an intramolecular process that is fast in comparison with the overall molecular tumbling, the relaxation rate constant is directly proportional to S^2, because intramolecular mobility leads to partial averaging of the relaxation-active dipolar coupling constants. The order parameter S^2 is calculated for each C atom from the populations p_1 and p_2 of the two corresponding conformers and the jump angle $\Delta\Theta$ according to the equation

$$S^2 = 1 - 3p_1p_2(\sin\Delta\Theta)^2 \quad (6)$$

The results are summarized in Table IV. The order parameters derived from the simulation are somewhat larger than the experimentally derived ones. This is a consequence of the slightly more asymmetric populations (p_1, p_2) of the two conformers and the slightly smaller jump angles $\Delta\Theta$ occurring in the simulation.

To study the influence of the friction coefficient on the proline ring flips, we determined the average residence times for each conformation of the four prolines. The residence time is defined as the time interval between two subsequent ring flips where ring flips are considered only when the χ_2 angle crosses the barrier at 0° by more than 10°. According to Kramers-modified transition state theory,[27,28] this restriction is necessary in stochastic dynamics because random collisions with the solvent can prevent the completion of an otherwise successful transition. Parts a and b of Figure 4 show the residence time distribution for Pro^2 and Pro^3. Table V collects the average residence times together with the largest observed residence time.

As can be seen from Table V, varying the friction coefficient between 19 and 100 ps^{-1} does not influence the residence time distribution much. Note that due to effective shielding from the solvent the weight factor for the accessible surface area is zero for most atoms in antamanide (see Figure 1). Only very few atoms at the periphery contribute to the friction. The mean weight factor for all atoms is as low as 0.07. Assigning to each atom a fixed friction coefficient of 20 ps^{-1} results in a mean atomic friction coefficient that is three times larger than that in run **B**. Still, the average and dynamical properties of the corresponding run **C** are very similar to those of runs **A** and **B**. We found that only solvent friction coefficients above 250 ps^{-1} result in an excessively viscous environment that causes considerable changes in the average and dynamical properties of antamanide.

Mádi et al.[10] have determined values for the effective correlation times for the proline puckering of Pro^2 and Pro^7 of the order of 30 and 36 ps, respectively. As the authors point out, these results have a large uncertainty due to relative insensitivity of the NMR relaxation times to the time scale of these fast motions. The average residence times we obtained from the simulations are significantly smaller than the correlation times obtained from NMR. Artificially increasing the residence times by increasing the friction coefficient in the simulations is in principle possible. However, the required 10-fold increase of the residence time would lead to an unphysical friction coefficient of the order of 1000 ps^{-1} for chloroform. Tentatively, we have increased the torsional barriers for the proline carbon–carbon bonds to increase the

(22) Karle, I. L.; Wieland, T.; Schermer, D.; Ottenheym, H. C. J. *Proc. Natl. Acad. Sci. U.S.A.* **1979**, *76*, 1532.
(23) Haasnoot, C. A. G.; Leeuw, F. A. A. M.; Altona, C. *Tetrahedron* **1980**, *36*, 2783.
(24) Haasnoot, C. A. G.; Leeuw, F. A. A. M.; Leeuw, H. P. M.; Altona, C. *Biopolymers* **1981**, *20*, 1211.
(25) Huggins, M. L. *J. Am. Chem. Soc.* **1953**, *75*, 4123.
(26) Haasnoot, C. A. G.; Leeuw, F. A. A. M.; Leeuw, H. P. M.; Altona, C. *Recl. Trav. Chim. Pays-Bas* **1979**, *98*, 576.
(27) Kramers, H. A. *Physica* **1940**, *7*, 284.
(28) van Gunsteren, W. F.; Berendsen, H. J. C.; Rullmann, J. A. C. *Mol. Phys.* **1981**, *44*, 69.

Table I. Population (p) of the Major Conformations and Average χ_2 Angles (in degrees) Found for the Major (M) and the Minor (m) Conformations of the Proline Residues for Four Backbone Conformations (I–IV) of Antamanide

	I			II			III			IV[a]		
		χ_2			χ_2			χ_2			χ_2	
	p	M	m	p	M	m	p	M	m	p	M	m
Pro^2	0.72	36	−31	0.70	36	−30	0.75	34	−31	0.72	35	−31
Pro^7	0.72	35	−31	0.72	34	−31	0.71	34	−31	0.77	35	−30
Pro^3	0.85	−32	24	0.81	−33	28	0.84	−33	27	0.83	−32	25
Pro^8	0.83	−31	24	0.78	−32	25	0.83	−33	27	0.83	−33	27

[a] The results for conformation IV (ϕ_5/ϕ_{10} = +64°/−75°) were obtained from a 300-ps trajectory of a separate simulation with a fixed friction coefficient (γ) value of 20 ps^{-1}.

Table II. Populations and Mean Torsional Angles[a] (in degrees) of the Observed Proline Conformations As Obtained from the Standard SD Simulation A together with Results from X-ray Analysis[22] (XR) and from NMR Spectroscopy[10]

	Pro^2					Pro^7					Pro^3					Pro^8			
	XR	NMR		SD		XR	NMR		SD		XR	NMR		SD		XR	NMR	SD	
p_i		0.65	0.35	0.75	0.25		0.55	0.45	0.71	0.29		0.90	0.10	0.84	0.16			0.83	0.17
ϕ	−64			−59	−62	−62			−58	−62	−80			−90	−85	−92		−88	−83
χ_0	−1	+4	−5	+8	−2	−10	−6	−8	+9	−2	−9	−15	−24	−20	−13	−16	−14	−19	−11
χ_1	−15	−30	+23	−26	+21	+11	−22	+26	−27	+20	+25	+35	−4	+32	−9	+29	+34	+32	−11
χ_2	+26	+45	−32	+34	−31	−11	+42	−34	+34	−31	−33	−42	+30	−33	+27	−31	−40	−33	+27
χ_3	−27	−42	+29	−29	+30	+6	−45	+29	−29	+30	+27	+33	−45	+21	−34	+23	+31	+22	−33
χ_4	+15	+24	−15	+13	−18	+3	+31	−13	+12	−18	−10	−11	+42	0	+29	−5	−10	−2	+28

[a] The root-mean-square values from the simulation vary between 7° and 12°.

Table III. Comparison of $^3J_{HH}$ Coupling Constants (in Hz) from NMR[10] and from SD Simulation A

	Pro^2		Pro^7		Pro^3		Pro^8	
^3J	NMR	SD	NMR	SD	NMR	SD	NMR	SD
$\alpha\beta_c$	8.0	7.8	8.8	7.8	8.5	7.9	8.1	8.0
$\alpha\beta_t$	7.4	7.8	5.8	7.5	1.1	2.3	0.9	2.4
$\beta_c\gamma_c$	7.1	8.3	7.4	8.3	6.8	8.7	6.8	8.7
$\beta_c\gamma_t$	4.8	3.2	5.9	3.6	12.0	9.8	13.0	9.7
$\beta_t\gamma_c$	9.0	9.0	7.5	8.5	2.4	2.2	1.4	2.3
$\beta_t\gamma_t$	7.1	8.4	7.0	8.4	6.5	8.6	6.4	8.5
$\gamma_c\delta_c$	7.6	8.2	7.3	8.2	7.6	8.7	7.3	8.6
$\gamma_c\delta_t$	8.5	8.0	7.4	7.6	2.1	3.4	1.5	3.4
$\gamma_t\delta_c$	4.6	3.6	5.4	3.9	10.3	7.6	10.9	7.7
$\gamma_t\delta_t$	7.0	8.0	7.0	8.1	8.5	8.9	8.8	8.8

Table IV. Jump Angles ($\Delta\Theta$, degrees) and Order Parameters (S^2) from NMR[10] and from SD Simulation A

		Pro^2		Pro^7		Pro^3	Pro^8
		NMR	SD	NMR	SD	SD	SD
p_1		0.65	0.75	0.55	0.71	0.84	0.83
p_2		0.35	0.25	0.45	0.29	0.16	0.17
$\Delta\Theta$	C_α–H	4	3	1	3	4	4
	C_β–H	50	44	44	44	40	41
	C_γ–H	75	64	76	65	58	59
	C_δ–H	35	30	41	29	27	27
S^2	C_α	0.997	0.998	1.00	0.998	0.998	0.998
	C_β	0.599	0.734	0.642	0.701	0.832	0.819
	C_γ	0.363	0.546	0.301	0.498	0.704	0.690
	C_δ	0.775	0.863	0.680	0.854	0.914	0.911

residence times and checked if, apart from the residence time distribution, the average and the dynamical properties still remained the same. For the angles χ_1, χ_2, and χ_3, the dihedral angle force constant was changed from 5.9 kJ mol^{-1} (ref 15) to 7.3 kJ mol^{-1}, and run A was repeated (A′). The average torsional angles as well as the populations for the two proline conformations remained well within the root-mean-square deviations of run A. As can be seen from Table V, the average residence times increased for Pro^2 and Pro^7 by factors of 4.4 and 3.7, respectively, while those for Pro^3 and Pro^8 increased by 2.2 and 2.5, respectively. This implies that another slight enlargement of the dihedral angle force constants will lead to residence times comparable to the experimental correlation times.

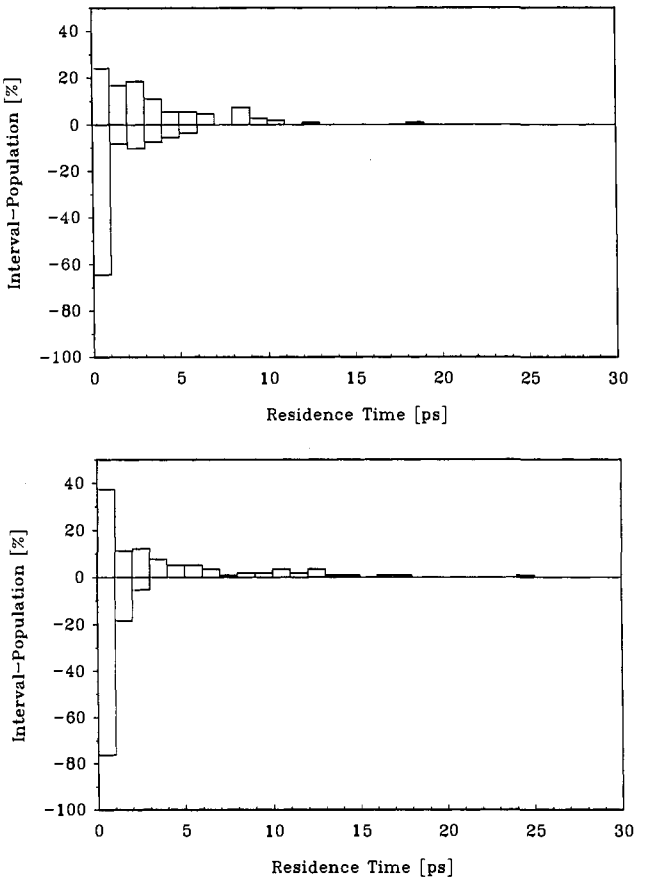

Figure 4. (a) Residence time distribution for the major (top) and the minor (bottom) conformers of Pro^2 from SD simulation A. (b) Residence time distribution for the major (top) and the minor (bottom) conformers of Pro^3 from SD simulation A.

4. Conclusions

The results demonstrate that stochastic dynamics simulations, which mimic a solution of antamanide in carbon tetrachloride and chloroform, can reproduce the conformational and dynamic properties of the proline residues as can be seen by comparing computed and measured populations and the $^3J_{HH}$ coupling

Table V. Largest Observed Lifetimes (τ_m, ps) and Average Residence Times (τ_r, ps) for the SD Simulations with Different Friction Coefficients (γ, ps^{-1})

		Pro^2				Pro^7				Pro^3				Pro^8			
		major		minor		major		minor		major		minor		major		minor	
run	γ	τ_m	τ_r	τ_m	τ_r	τ_m	τ_r	τ_m	τ_r	τ_m	τ_r	τ_m	τ_r	τ_m	τ_r	τ_m	τ_r
A	19	19	3.4	6	1.2	17	3.6	9	1.6	25	3.7	3	0.6	32	3.7	4	0.7
B	100	18	4.6	13	2.0	16	3.1	12	2.0	26	3.5	4	0.7	31	4.3	4	0.8
C	20[a]	19	4.3	12	1.4	27	4.6	10	1.8	28	3.3	3	0.7	29	3.7	5	0.8
A′	19[b]	56	14.6	27	5.5	75	13.1	37	6.1	41	8.0	11	1.4	85	7.8	10	2.0

[a] A fixed accessible area weight factor of 1 is applied. [b] With increased rotational barrier for χ_1, χ_2, and χ_3.

constants. Similar to the NMR results, the residues Pro^2 and Pro^7 flip in the simulation between two energetically similar conformations with geometries almost identical to those obtained from NMR. Also the order parameters S^2 are well-reproduced. For residues Pro^3 and Pro^8, the computed populations of the minor conformations are below 20% and are difficult to detect by NMR. For Pro^3, a population ratio of 90:10 was proposed on the basis of the NMR data.[10] Although Pro^3 and Pro^8 show dynamics, the less populated conformation must energetically be unfavorable. The lifetimes for these conformations are very short, usually less than 2 ps.

The lifetimes for the Pro^2 and Pro^7 conformations are longer. By comparison with the results from NMR, where average residence times in the order of 30 ps were found, the average residence times of 4 ps obtained from the simulation are too small. These results imply that the GROMOS force field is somewhat too flexible in the case of the proline rings. The residence times can be increased by raising the rotational barrier for the χ_1, χ_2, and χ_3 angles within the prolines by a few kilojoules per mole without affecting the equilibrium conformations. However, our simulated results agree well with the results of Sarkar and co-workers,[29,30] who analyzed *cyclo*-(Gly-Pro-D-Ala)$_2$,[29] proline, and proline hydrochloride[30] in the solid state by NMR spectroscopy and determined the correlation times for the fast ring flips to be in the order of 12, 1.3, and 0.3 ps, respectively, assuming a simple, equally populated two-state model.

Finally, we note that the dynamics of the proline ring flips are not affected by the magnitude of the friction coefficient as long as it is chosen within an order of magnitude of the value corresponding to the actual viscosity of carbon tetrachloride. The proline dynamics appears to be insensitive to the equilibrium conformational dynamics of the peptide ring that has been observed in the experiment as well as in the initial phase of the dynamics simulation.

This paper shows that the simplicity of the united-atom approach used in GROMOS does not impede the achievement of realistic structures and dynamics in a conformational equilibrium.

Acknowledgment. Discussions with Jürgen Schmidt are gratefully acknowledged. This research has been supported in part by the Swiss National Science Foundation.

(29) Sarkar, S. K.; Torchia, D. A.; Kopple, K. D.; VanderHart, D. L. *J. Am. Chem. Soc.* **1984**, *106*, 3328.
(30) Sarkar, S. K.; Young, P. E.; Torchia, D. A. *J. Am. Chem. Soc.* **1986**, *108*, 6459.